Single Switch ZCS Resonant Converter with High Step-up Ratio

Jaeyeon Lee, Minjae Kim, Hyeonju Jeong and Sewan Choi, *IEEE Senior Member*
Department of Electrical and Information Engineering
Seoul National University of Science and **Tech**nology
Email: schoi@seoultech.ac.kr

***Abstract*— This paper proposes a high step-up resonant converter which is suitable for low power application. The proposed converter is simple in structure since it employs only one switch while not necessitating clamp circuit. Also, the proposed converter is able to achieve ZCS turn-on and turn-off of switch and ZCS turn-off of diodes, resulting in high efficiency. Furthermore, the proposed converter has reduced transformer volume due to guaranteed zero dc-offset current in transformer. Experimental results on 250W prototype are provided to validate the proposed concept.**

Keywords—single switch, soft switching, high step up, resonant converter

I. INTRODUCTION

The demand for isolated high step-up dc-dc converters has gradually been increasing in accordance with the growth in photovoltaic module-integrated converter (MIC) system, portable fuel cell system and vehicle inverter where high efficiency, high power density and low cost are required.

The high step-up dc-dc converter has two types: passive clamped [1] and active-clamped [2]-[4]. The passive clamped converter has simple structure and small switch count, but suffers from excessive power losses associated with hard switching of main switch. Also, the RCD snubber circuit of the passive clamped converter cause large amount of losses. Active-clamped converters have actively been developed based on three basic topologies: push–pull [2], full-bridge [3], and half-bridge [4]. They achieve not only lossless clamping of voltage spikes caused by transformer leakage inductance but also zero-voltage switching (ZVS) turn-on of switches. However, it seems not to achieve high efficiency and low cost in relatively low power application since they employ at least four switches and gate driver circuits.

In response to this concern, single switch isolated dc-dc converters have been proposed for low power application [5]-[11]. Single switch isolated dc–dc converters could be PWM converters [5]-[6] such as Z-source converter and flyback converter or resonant converters [9]-[11] such as CL, LCL and CLL resonant converter. The Z-source converter [5] and flyback converter [6] are hard switched at both turn-on and turn-off instants. Frequency-controlled flyback converter [7] and series-connected forward-flyback converter [8] achieve zero-current switching (ZCS) turn-on of switch, but the switch is hard switched at turn-off instant. In contrast, resonant converters have many advantages such as the following: 1) soft switching turn-on and turn-off of switch; 2) utilization of parasitic elements such as leakage and/or magnetizing inductor of transformer as resonant elements; 3) simple structure due to absence of clamp circuits. However, the aforementioned single switch topologies have large dc-offset current in the transformer leading to increased transformer volume.

In this paper, a single switch ZCS resonant converter is proposed for high step-up application. The proposed converter has the following features: 1) reduced transformer volume due to zero dc-offset current in transformer; 2) simple structure due to absence of clamp circuits; 3) ZCS turn-on and turn-off of switch regardless of voltage and load variation; and 4) ZCS turn-off of all diodes leading to negligible voltage surge associated with the diode reverse recovery. These features make it possible to achieve high efficiency and low cost in the low power, high step-up application. Experimental results on 250W prototype are provided to validate the proposed concept.

II. PROPOSED CONVERTER

Fig. 1 shows the circuit diagram of the proposed converter; it consists of input filter L_i, switch S_1, clamp capacitor C_C at the transformer primary side and L_r-C_r parallel resonant tank and voltage doubler rectifier at the transformer secondary side. The output voltage of the proposed converter is regulated by switching frequency variation.

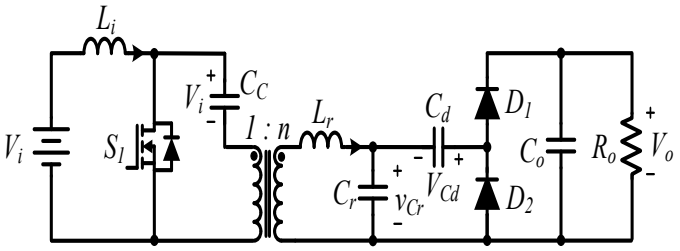

Fig. 1: Circuit diagram of the proposed converter.

978-1-5090-1210-7/16/$31.00 ©2016 IEEE

A. Operating Principle

Fig. 2 and 4 show key waveforms and operation states of the proposed converter, respectively. In order to simplify the analysis of the steady-state operation, it is assumed that the input filter inductance is large enough so that it can be treated as a constant current source during a switching period. It is also assumed that C_C, C_d and C_o are large enough so that they can be treated as constant voltage sources during a switching period. The average voltage across C_C is the same as the input voltage V_i. The operation states of the proposed converter are described as follows.

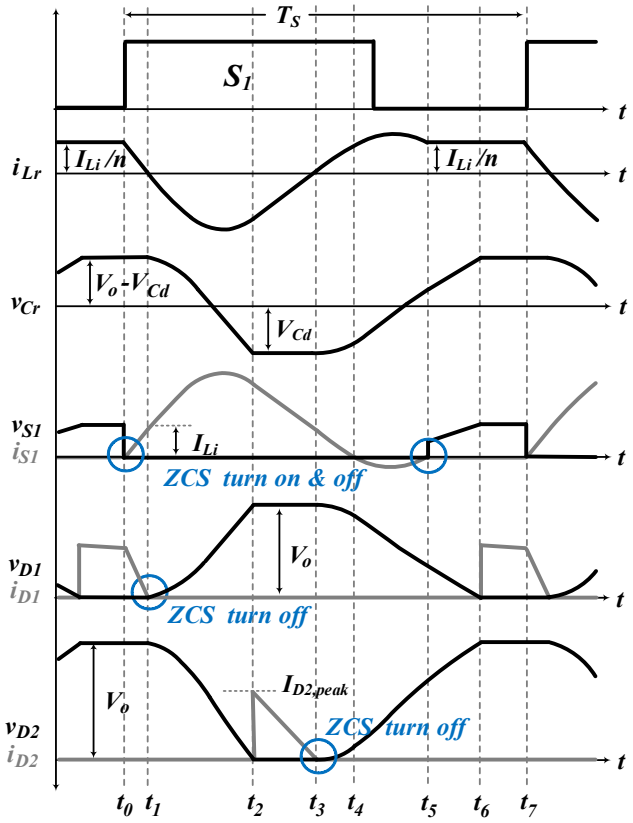

Fig. 2. Key waveforms of the proposed converter.

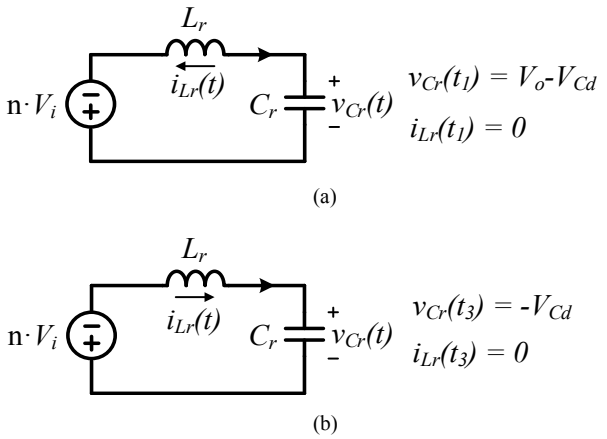

Fig. 3. Equivalent resonant circuit. (a) Mode 2

(b) Mode 4 and Mode 5

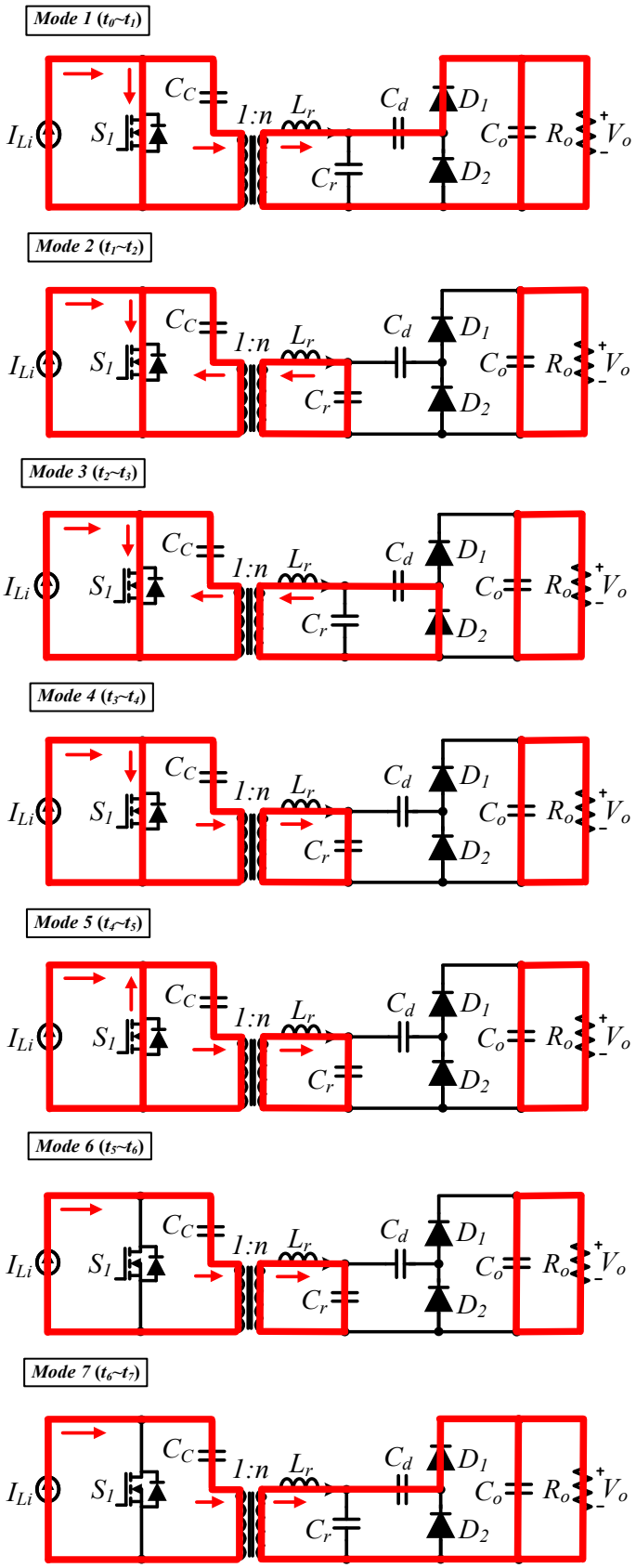

Fig. 4. Operation states of the proposed converter.

Mode 1[t_0 ~ t_1]: This mode begins when switch S_1 is turned on at t_0. Then, current i_{Lr} decreases linearly and can be expressed by

$$i_{Lr}(t) = \frac{I_{Li}}{n} - \frac{nV_i + V_o - V_{Cd}}{L_r}(t - t_0) \qquad t_0 < t < t_1 \quad (1)$$

This leads to ZCS turn off of diode D_1. The switch current also increases linearly, making switch S_1 to be turned on with ZCS. This mode ends when current i_{Lr} reaches 0A.

Mode 2[t_1 ~ t_2]: This mode begins when current i_{Lr} changes its directions. Since diode D_2 is reverse biased, L_r and C_r start resonating with the equivalent circuit shown in Fig. 3(a). The voltage and current of resonant components are determined, respectively, as follows:

$$i_{Lr}(t) = (-nV_i - V_o + V_{Cd})\sqrt{\frac{C_r}{L_r}}\sin(\omega_r(t - t_1)) \qquad t_1 < t < t_2 \quad (2)$$

$$v_{Cr}(t) = (nV_i + V_o - V_{Cd})\cos(\omega_r(t - t_1)) - nV_i \qquad t_1 < t < t_2 \quad (3)$$

where $\omega_r = 1/\sqrt{L_r C_r}$. The resonant operation continues until voltage v_{Cr} becomes equal to -V_{Cd}.

Mode 3[t_2 ~ t_3]: Diode D_2 is turned on at t_2 when v_{Cr} reaches -V_{Cd}. Then, current i_{Lr} decreases linearly and can be expressed by

$$i_{Lr}(t) = i_{Lr}(t_2) - \frac{nV_i - V_{Cd}}{L_r}(t - t_2) \qquad t_2 < t < t_3 \quad (4)$$

This leads to ZCS turn-off of diode D_2. This mode ends when current i_{Lr} reaches 0A.

Mode 4[t_3 ~ t_4]: This mode begins when current i_{Lr} changes its directions at t_3. Since diode D_1 is reverse biased, L_r and C_r start resonating with equivalent circuit shown in Fig. 3(b). The voltage and current of resonant components are determined, respectively, as follows:

$$i_{Lr}(t) = (-nV_i + V_{Cd})\sqrt{\frac{C_r}{L_r}}\sin(\omega_r(t - t_3)) \qquad t_3 < t < t_5 \quad (5)$$

$$v_{Cr}(t) = (nV_i - V_{Cd})\cos(\omega_r(t - t_3)) - nV_i \qquad t_3 < t < t_5 \quad (6)$$

This mode ends when current i_{Lr} reaches I_{Li}/n.

Mode 5[t_4 ~ t_5]: At time t_4 the current through switch S_1 changes its direction, flowing through main channel of switch S_1 since the gating signal for switch S_1 is still applied. The current flows through the body diode of switch S_1 when switch S_1 is turned off. It is noted that switch S_1 is turned off with ZCS due to the L_r-C_r resonance. The resonant operation continues until current i_{Lr} becomes again equal to I_{Li}/n.

Mode 6[t_5 ~ t_6]: During this mode, switch S_1 is in the turn-off state and the constant current flows through the primary winding of the transformer. Voltage v_{Cr} increases linearly and can be expressed by

$$v_{Cr}(t) = \frac{I_{Li}}{nC_r}(t - t_5) + v_{Cr}(t_5) \qquad t_5 < t < t_6 \quad (7)$$

This mode continues until voltage v_{Cr} reaches V_o-V_{Cd}.

Mode 7[t_6 ~ t_7]: At time t_6 diode D_1 is turned on and the input power is transferred to the output side. This mode ends when switch S_1 is turned on at time t_7.

B. Volatage Gain Expression

To obtain voltage gain of the proposed converter, voltages across C_C and C_d are assumed to be constant.

From Fig. 2, we have

$$t_7 - t_0 = T_S \quad (8)$$

The time interval from t_0 to t_1 in Fig. 2 can be obtained from (1) by

$$t_1 - t_0 = \frac{I_{Li}L_r}{n(nV_i + V_o - V_{Cd})} \quad (9)$$

The time interval from t_1 to t_2 in Fig. 2 can be obtained from (3) by

$$t_2 - t_1 = \frac{1}{\omega_r}\arccos\left(\frac{nV_i - V_{Cd}}{nV_i + V_o - V_{Cd}}\right) \quad (10)$$

Since the average current of diode D_2 is identical to the average load current in the steady state, the following equation is obtained:

$$I_{D2,avg} = \frac{V_o}{R_o} = \frac{1}{2}I_{D2,peak}(t_3 - t_2)/T_S \quad (11)$$

From (4), we have

$$\frac{V_{Cd} - nV_i}{L_r} = \frac{I_{D2,peak}}{t_3 - t_2} \quad (12)$$

From (11) and (12), current $I_{D2,peak}$ can be obtained by

$$I_{D2,peak} = \sqrt{\frac{2V_o(V_{Cd} - nV_i)}{R_o L_r f_S}} \quad (13)$$

Applying trigonometric function to (2), (3) and (13), voltage V_{Cd} can be obtained by

$$V_{Cd} = nV_i + \frac{R_o f_S C_r V_o}{2(1 + R_o f_S C_r)} \quad (14)$$

The time interval from t_2 to t_3 in Fig. 2 can be obtained from (12) and (13) by

$$t_3 - t_2 = \sqrt{\frac{2V_o L_r}{R_o f_S (V_{Cd} - nV_i)}} \quad (15)$$

The time interval from t_3 to t_5 in Fig. 2 can be obtained from (5) by

$$t_5 - t_3 = \frac{\pi}{\omega_r} - \frac{1}{\omega_r}\arcsin\left(\frac{I_{Li}}{n(V_{Cd}-nV_i)}\sqrt{\frac{L_r}{C_r}}\right) \quad (16)$$

The time interval from t_5 to t_6 in Fig. 2 can be obtained from (6), (7) and (16) by

$$t_6 - t_5 = \frac{nC_r}{I_{Li}}\left(V_o - V_{Cd} + nV_i - \sqrt{(V_{Cd}-nV_i)^2 - \frac{L_r}{C_r}\left(\frac{I_{Li}}{n}\right)^2}\right) \quad (17)$$

Since the average current of diode D_1 is identical to the average load current in the steady state, the following equation is obtained:

$$I_{D1,avg} = \frac{V_o}{R_o} = \frac{I_{Li}}{2n}\left((t_1 - t_0) + 2(t_7 - t_6)\right)/T_S \quad (18)$$

The time interval from t_6 to t_7 in Fig. 2 can be obtained from (9) and (18) by

$$t_7 - t_6 = \frac{nV_oT_S}{R_oI_{Li}} - \frac{I_{Li}L_r}{2n(nV_i + V_o - V_{Cd})} \quad (19)$$

From (8)-(10), (14)-(17) and (19), the voltage gain can be obtained by (20)

Where $M = V_o/V_i$, $k = R_oC_rf_s$, $\omega_r = 1/\sqrt{L_rC_r}$, $T_S = 1/f_s$ and $Z = \sqrt{L_r/C_r}$

Fig. 5 shows the curves of the voltage gain plotted over frequency for different values of *n*.

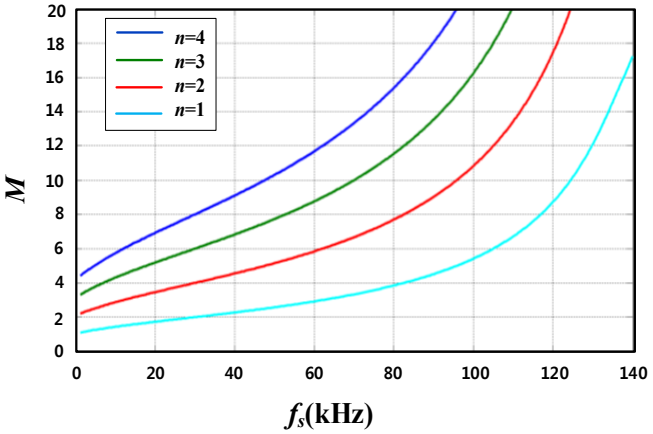

Fig. 5. Voltage gain of the proposed converter at different values of n

III. SIMULATION AND EXPERIMENTAL RESULTS

A 250W prototype of the proposed converter has been built and tested to verify the operating principle, and the simulation and experimental results are provided. The system specification used in the experiment is as follows:

- Output power P_o = 250W;
- Input voltage V_i = 28~38V;
- Output voltage V_o = 380V;
- Turn ratio $n_1 : n_2$ = 1 : 2;
- Resonant inductor L_r = 16uH;
- Resonant capacitor C_r = 40nF;

Fig. 6 shows the simulated steady-state waveforms at the output power of 250W. Fig. 7-8 show the experimental waveforms under different output power. It is seen from simulation and experimental results that switch S_1 is turned ON and OFF with ZCS and diodes D_1 and D_2 are turned OFF with ZCS, respectively, due to the resonant components. Fig. 7-8 show the experimental waveforms of current i_{Cr} and voltage v_{Cr} which are also determined by resonant components.

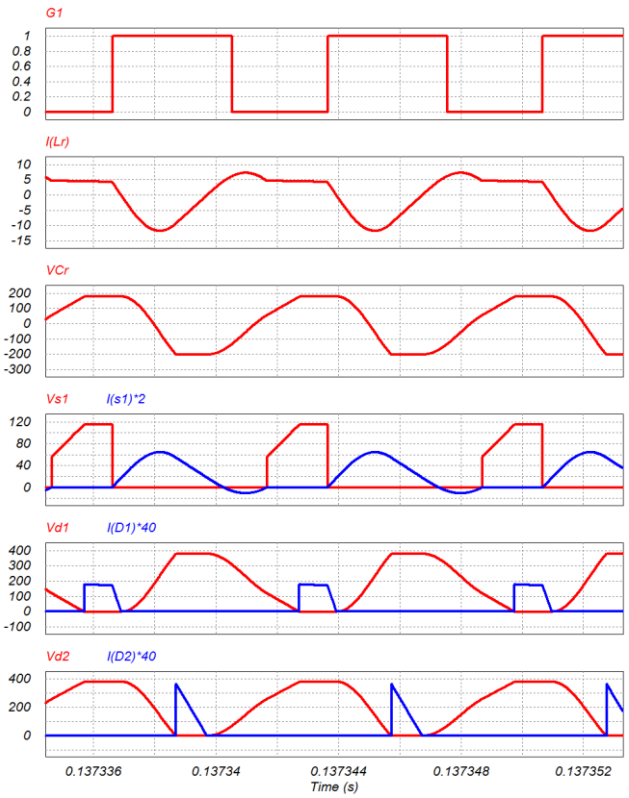

Fig. 6. Simulation waveforms at V_i=28V and P_o=250W.

$$M = \frac{n\left(k\left(\frac{2+k}{2(1+k)} - \sqrt{\frac{k^2}{4(1+k)^2} - \frac{Z^2M^2}{n^2R_o^2}}\right)+1\right)}{\left(1 - \frac{L_rMf_s(1+k)}{nR_o(2+k)} + \frac{f_s}{\omega_r}\arccos\left(\frac{k}{2+k}\right) - 2\sqrt{\frac{L_rf_s(1+k)}{R_ok}} - \frac{2\pi f_s}{\omega_r} + \frac{f_s}{\omega_r}\arcsin\left(\frac{2MZ(1+k)}{nkR_o}\right)\right)} \quad (20)$$

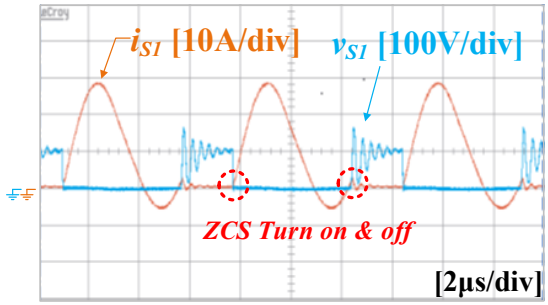

(a)

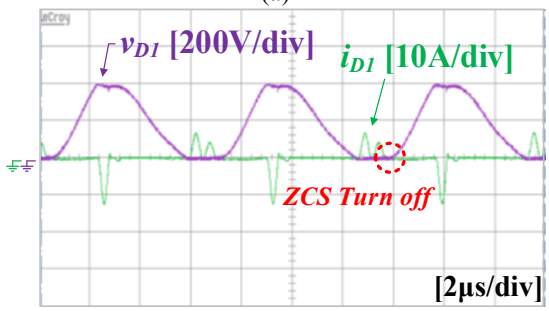

(b)

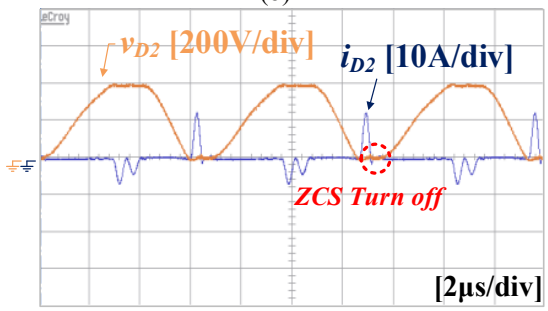

(c)

Fig. 7. Experimental waveforms at V_i=28V and P_o=150W: (a) v_{S1} and i_{S1}. (b) v_{D1} and i_{D1}. (c) v_{D2} and i_{D2}

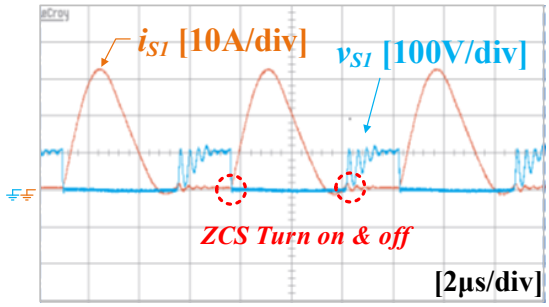

(a)

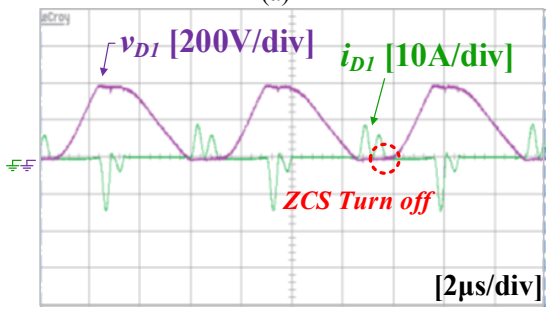

(b)

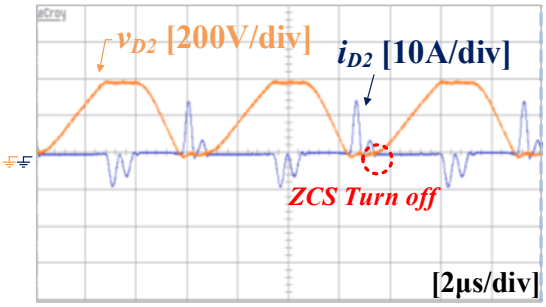

(c)

Fig. 8. Experimental waveforms at V_i=28V and P_o=250W: (a) v_{S1} and i_{S1}. (b) v_{D1} and i_{D1}. (c) v_{D2} and i_{D2}

IV. Conclusion

In this paper, a single switch resonant converter is proposed for high step-up application such as MIC, portable fuel cell, and vehicle inverter. The proposed converter has simple structure due to absence of clamp circuits. Due to zero dc-offset current of the transformer, the transformer volume of the proposed converter is small compared to the conventional flyback based single switch converter. Further, the proposed converter achieves ZCS turn-on and turn-off of the switch and ZCS turn-off of all diodes regardless of voltage and load variation. Experimental results from a 250W prototype are provided to validate the proposed concept.

Acknowledgment

This work was supported by the National Research Foundation of Korea (NRF) grant funded by the Korea Government (MISP) (2014R1A2A2A01003724).

References

[1] D. A. Ruiz-Caballero and I. Barbi, "A new flyback-current-fed push-pull DC-DC converter," IEEE Trans. Power Electron., vol. 14, no. 6, pp. 1056–1064, Nov. 1999J. Clerk Maxwell, A Treatise on Electricity and Magnetism, 3rd ed., vol. 2. Oxford: Clarendon, 1892, pp.68-73.

[2] F. J. Nome and I. Barbi, "A ZVS clamping mode-current-fed push–pull DC–DC converter," in Proc. IEEE Int. Symp. Ind. Electron., vol. 2, 1998, pp. 617–621.

[3] V. Yakushev, V. Meleshin, and S. Fraidlin, "Full-bridge isolated current fed converter with active clamp," in Proc. IEEE Appl. Power Electron. Conf. Expo., vol. 1, 1999, pp. 560–566.

[4] S. Han, H. Yoon, G. Moon, M. Youn, Y. Kim, and K. Lee, "A new active clamping zero-voltage switching PWM current-fed half-bridge converter," IEEE Trans. Power Electron., vol. 20, no. 6, pp. 1271–1279, Nov. 2005.

[5] F. Evran and M. T. Aydemir, "Z-source-based isolated high step-up converter," IET Power Electron., vol. 6, no. 1, pp. 117–224, Jan. 2013.

[6] J. H. Lee, T. J. Liang, and J. F. Chen, "Isolated coupled-inductor-integrated DC-DC converter with nondissipative snubber for solar energy applications," IEEE Trans. Ind. Electron., vol. 61, no. 7, pp. 3337–3348, Jul. 2014.

[7] J.-M. Kwon, W.-Y. Choi, and B.-H. Kwon, "Single-switch quasi-resonant converter," IEEE Trans. Ind. Electron., vol. 56, no. 4, pp. 1158–1163, Apr. 2009.

[8] J.-H. Lee, J.-H. Park, and J. H. Jeon, "Series-connected forward-flyback converter for high step-up power conversion," IEEE Trans. Power Electron., vol. 26, no. 12, pp. 3629–3641, Dec. 2011.

[9] A. Emrani, E. Adib, and H. Farzanehfard, “Single-switch soft-switched isolated DC-DC converter,” IEEE Trans. Power Electron., vol. 27, no. 4, pp. 1952–1957, Apr. 2012.

[10] Jianwu Zeng, Wei Qiao, and Liyan Qu, “LCL-resonant single-switch isolated DC–DC converter,” IET in Power Electronics, vol.8, no.7, pp.1209-1216, Jul. 2015.

[11] Seung-Hee Ryu, Jung-Hoon Ahn, Kwang-Seung Cho, and Byoung-Kuk Lee, “Single-switch ZVZCS quasi-resonant CLL isolated DC-DC converter for 32″ LCD TV,” Journal of Electrical Engineering & Technology, vol. 10, no. 4, pp.1646-1654, Jul. 2015.